



Article

Investigation on the Optical Design and Performance of a Single-Axis-Tracking Solar Parabolic trough Collector with a Secondary Reflector

Chinnasamy Subramaniyan ¹, Jothirathinam Subramani ², Balasubramanian Kalidasan ¹, Natarajan Anbuselvan ³, Thangaraj Yuvaraj ³, Natarajan Prabaharan ^{4,*} and Tomonobu Senju ^{5,*}

¹ Department of Mechanical Engineering, Bannari Amman Institute of Technology, Sathyamangalam 638401, India; subra.csm@gmail.com (C.S.); kalidasancinna@gmail.com (B.K.)

² Chennai SSSS Equipments Private Limited, Chennai 600077, India; jsubramani.phd@gmail.com

³ Department of Electrical and Electronics Engineering, Saveetha School of Engineering, Saveetha Institute of Medical and Technical Sciences, Saveetha University, Chennai 602105, India; anbu.1324@gmail.com (N.A.); yuvaraj4252@gmail.com (T.Y.)

⁴ Department of Electrical and Electronics Engineering, SASTRA Deemed University, Thanjavur 613401, India

⁵ Department of Electrical and Electronics Engineering, University of the Ryukyus, Okinawa 903-0213, Japan

* Correspondence: prabaharan.nataraj@gmail.com (N.P.); b985542@tec.u-ryukyu.ac.jp (T.S.)



Citation: Subramaniyan, C.; Subramani, J.; Kalidasan, B.; Anbuselvan, N.; Yuvaraj, T.; Prabaharan, N.; Senju, T.

Investigation on the Optical Design and Performance of a Single-Axis-Tracking Solar Parabolic trough Collector with a Secondary Reflector. *Sustainability* **2021**, *13*, 9918.

<https://doi.org/10.3390/su13179918>

Academic Editor: Luca Cioccolanti

Received: 14 July 2021

Accepted: 30 August 2021

Published: 3 September 2021

Publisher's Note: MDPI stays neutral with regard to jurisdictional claims in published maps and institutional affiliations.



Copyright: © 2021 by the authors. Licensee MDPI, Basel, Switzerland. This article is an open access article distributed under the terms and conditions of the Creative Commons Attribution (CC BY) license (<https://creativecommons.org/licenses/by/4.0/>).

Abstract: The design of solar concentrating collectors for the effective utilization of solar energy is a challenging condition due to tracking errors leading to different divergences of the solar incidence angle. To enhance the optical performance of solar parabolic trough collectors (SPTC) under a diverged solar incidence angle, an additional compound parabolic concentrator (CPC) is introduced as a secondary reflector. SPTC with CPC is designed and modeled for a single axis-tracking concentrating collector based on the local ambient conditions. In this work, the optical performance of the novel SPTC system with and without a secondary reflector is investigated using MATLAB and TRACEPRO software simulations for various tracking errors. The significance parameters such as the solar incidence angle, aperture length, receiver tube diameter, rim angle, concentration ratio, solar radiation, and absorbed flux are analyzed. The simulation results show that the rate of the absorbed flux on the receiver tube is significantly improved by providing the secondary reflector, which enhances the optical efficiency of the collector. It is found that the optical efficiency of the SPTC with a secondary reflector is 20% higher than the conventional collector system for a solar incidence angle of 2°. This work can effectively direct the choice of optimal secondary reflectors for SPTC under different design and operating conditions.

Keywords: solar parabolic trough collector; solar compound parabolic collectors; rim angle; secondary concentrators; absorbed flux; incidence angle

1. Introduction

Renewable energy resources are the primary form of alternative energy for fossil fuels. Among the various resources of renewable energy, solar energy is the main form of alternative energy for fossil fuels. In addition, it provides a healthy and clean environment with economic and ethical benefits to the world. Due to depleted sources in fossil fuels and their environmental impacts, the researchers focus on the utilization of alternative energy sources such as solar energy as primary energy. There are numerous solar thermal systems available that can be applied for many processing industries and electrical power generation applications [1]. The solar parabolic trough collector is a type of solar thermal collector that is used to heat the working fluid. It can be realistic for low, medium, and high-temperature applications due to its nature of focused tube heating arrangement. Hence, it attracts many researchers to focus on the performance study and enhancement of the performance of SPTC [2,3].

Energy and economic analyses of SPTC with different working fluids have been done on the stationary concentrating collector in [4]. The optical and thermal efficiency has been identified as a maximum when the solar incidence angle was close to zero [4]. A blended plasmonic nanofluid partial coating has been introduced for the thermal performance investigation of SPTC [5]. In addition, the reflective metallic layer coating has been provided over the upper half part of the inner tube to reduce the emissivity losses. This investigation has been proved that the receiver tube diameter of a coated receiver tube can be increased without compensating the thermal efficiency of the system [5]. A cost-effective SPTC system has been developed in [6] that consists of a heat pipe as a receiver tube for the effective heat transfer medium and uses nanofluid as a working fluid. An investigation indicated that the maximum thermal efficiency of the SPTC was 76%, which was 4.7% higher than the evacuated tube collector [6]. Several works have been done in the field of alternative designs of SPTC for performance enhancement in various thermal applications. To evaluate the performance of an SPTC, it is necessary to conduct a study on the thermal performances of SPTC.

The parametric study of SPTC consists of mass flow rate optimization, concentration ratio, different heat transfer fluid, solar radiation, and heat gain [7]. A star-shaped insert has been fixed inside the receiver tube for enhancing the thermal performance of the SPTC and a maximum enhancement of 1% was achieved on the thermal performance of the SPCT with the optimized working conditions. The pressure drop due to inserts was also optimized for its compensation with respect to the increment on the thermal performances [8]. A novel S-curved sinusoidal-shaped twisted insert has been fixed inside the receiver tube, and the same setup has been tested for its thermal performance enhancement in SPTC. The thermal performance with respect to the three dimensions, the average Nusselt number, and the average friction coefficient was analyzed for the SPTC with inserts, and the results were compared with the base-collector without inserts [9]. The investigation on focusing the effect of geometrical parameters (aperture area, rim angle, focal length, and absorber diameter) and on enhancing the performance of the SPTC system was conducted to identify its optimal design and operating conditions [10]. Many alternative designs of the SPTC were investigated for their optical (tracking, selective coatings, and secondary reflectors) and thermal performance enhancements (working fluids, tabulators) [11]. Investigations have also been conducted on the performance of SPTC by varying the normal radiation, solar incidence angle, rim angle, aperture, and concentration ratio for improving the performance of the system. The effect of optical parameters was also studied for evaluating the impact of various optical properties on the performance of the solar system with different receiver tubes [12].

The performance of the SPTC has been analyzed for investigating the significance of having an arc-shaped linear cavity receiver tube, and the results indicated that the novel receiver tube provided better performance than the evacuated tube collectors [13]. An experimental investigation has been done on a solar parabolic trough air collector for improving thermal performance by providing the extended surfaces across receiver tube surfaces. The results show that the heat transfer rate between the tube and the air was significantly improved, and the exergy efficiency was increased by 2 to 4% using the pin fins in the collector receiver tube [14]. The improvement in the thermal performance of the SPTC with a larger aperture and concentration ratio has been tested with wire coil inserts. The contribution of wired coil inserts in the thermal performance of SPTC leads to 83% higher performance than the plain tubes without inserts [15]. The performance of CPC with and without nanoparticle filled porous on receiver tube has been comparatively studied, and the heat transfer characteristics were investigated. The result indicated that the Nusselt number has maximum for larger values of the volume fraction of nanoparticles [16]. The significance of effective design and operating strategies on the performance of CPC was also numerically and experimentally studied for various applications. The economic and technical feasibility of the improvement on the design and operating conditions of CPC collectors for better optical efficiency was also briefly discussed [17]. Few studies have

been made by varying the rim angles to obtain the highest optical performance of the CPC stationary concentrating collector or for improving the thermal performance of CPC collector [18]. An industrial purpose solar CPC collector has been tested for its thermal performance for a total heat load of 320,640 kWh. The heat losses and other accountable and unaccountable losses from the system were investigated for different ambient working conditions. The minimum and maximum range of the difference between the actual and expected heat loss was found to be 9 to 14.7% for the installed system [19]. There is numerous ongoing research to enhance the optical and thermal performance of SPTC and to reduce its optical losses by providing alternative designs, working fluids, and operating conditions [20]. The various reflective materials and their selective coatings for enhancing the optical performance of the SPTC solar systems were studied. The influence of the reflectivity on the thermal performance of SPTC has been briefly discussed and the performance of SPTC using silver and aluminum as a reflecting material has been comparatively studied for its better performance [21].

A novel vertical secondary booster reflector for SPTC has been introduced to enhance the optical performance of the solar collector for reducing the end optical losses. Nearly 21% of the optical performance has been enhanced through this secondary vertical booster [22]. An innovative design method for analyzing the performance of a large aperture two-stage SPTC has been developed and the result has shown that the optical efficiency of the base-collector was significantly increased by 5% by providing the secondary reflector [23]. The effect of gravity load and wind effect on the optical performance of the SPTC has been studied, and the significance of weight reduction on the tracking power consumption has also been studied for its better economic situations [24]. An investigation on the transient thermal performance of SPTC has been conducted using a mathematical model for experimental data collected from the 600-m-long SPTC collectors. Both the optical and thermal performance of the system have been investigated for better output with respect to various operating conditions [25]. An experimental study has been carried out for finding the effect of the absorber tube displacement in parabolic trough collectors using a novel approach with respect to the vertical and lateral displacement of the tubes [26]. The optical losses have been investigated for different design and operating parameters of solar collectors with the secondary reflectors. The effect of different absorber tubes at different shapes on the thermal performance of the solar collectors has been investigated for performance enhancement [27]. The investigation on thermal performance has been carried out to find the convective heat losses from a solar parabolic secondary receiver for a solar linear Fresnel reflector system. A numerical analysis has been performed on the system performance with respect to the aperture length, the acceptance angle, the focus point, the height of the secondary collector, and the distance of the focus point [28]. A study on the thermal performance and optical performance of a medium-temperature parabolic trough collector has been executed in the SPTC. The dirty factor for optical losses due to dust deposition was studied, and it was found that the instantaneous efficiency of the system falls by 13% [29]. Experimental investigation has been carried out for evaluating the optical losses due to the tracking error of a low-temperature and low concentration ratio SPTC. The significance of the tracking error angle on the performance of the SPTC has been investigated and it was found that the range of yearly maximum optical losses was 8.5% due to tracking errors [30].

Although numerous research work has been carried out to enhance the performance of SPTC by focused alternative designs, working fluids, receiver tubes, reflecting materials, selective coatings, and varying operating conditions, it can be clearly observed that a gap exists in analyzing the performance of SPTC by introducing a secondary reflector. To deal with optical losses due to the tracking error, a unique attempt is made by using a secondary reflector. The investigation is performed to evaluate and improve the optical performance of the single-axis-tracking SPTC system with secondary reflector for various tracking errors. A single-axis-tracking SPTC with CPC secondary reflector is designed, modeled, and simulated in MATLAB and TRACEPRO software for its improved performance. A

comparative analysis is performed among the design and operating parameters to identify the technical feasibility of providing the secondary reflector for SPTC with different solar incidence angles due to the tracking error.

2. Design of Parabolic trough Collector as a Primary Reflector

SPTC is a solar-concentrating thermal collector in which a circular receiver tube runs through the focal line of the parabola trough reflector. The reflector is oriented towards the sunlight at a normal angle (90°) to its base. Thus, the solar rays are exactly reflected towards the receiver tube at the focus line. The receiver tube contains the working fluid, which is heated to a high temperature at the outlet of the tube due to the concentration of reflected solar rays from the reflector to the surface of the absorber tube. The design and modeling of the SPTC totally depends on the rim angle, aperture, focus length, acceptance angle, depth distance, arc length, receiver tube diameter, and concentration ratio. However, the design of the majority of SPTC investigations are aiming to attain a higher concentration ratio for the better outlet temperature of working fluids. Similarly, the single-axis tracking mechanism is assumed to be a faultless one for the solar tracking conditions. The incidence angle of the solar rays is presumed to be 0° all the time since the tracking is always functioning in a faultless manner. However, practically, the solar rays are not exactly hitting the reflector trough at a normal angle due to the error in the tracking mechanism. The incidence angle of the solar rays is assumed to be the acceptance angle for the design of SPTC. If the system does not have any deviation on the solar incidence angle means, the solar acceptance angle of the SPTC is considered as 0° . If the maximum deviation in the system due to the error in tracking about 3° means, it is considered that the solar acceptance angle of the SPTC is 3° . Similarly, the solar incidence angle on the negative vector direction is also to be considered for the design, which is shown in Figure 1.

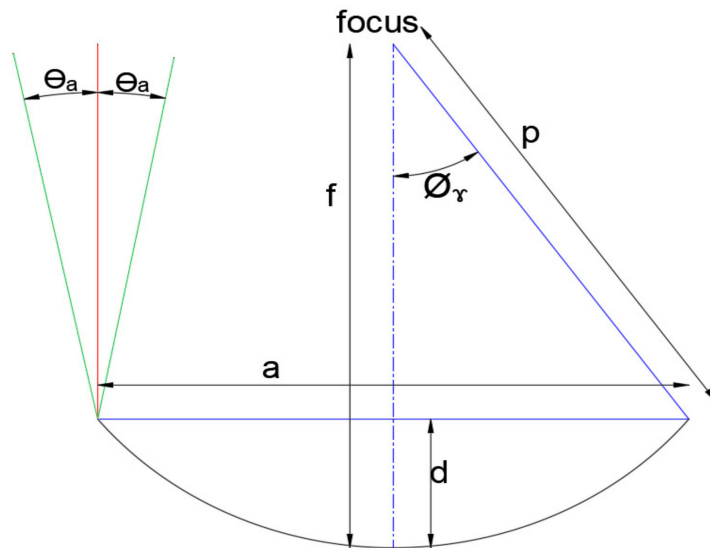


Figure 1. Geometrical design of the SPTC.

The mathematical model of the design of a parabolic trough collector as a primary reflector of the SPTC is derived for the incidence angle (0 to 3°) of solar rays due to the error in the tracking mechanism. The focus length and receiver diameter of the parabolic primary collector of SPTC are given by Equations (1) and (2), respectively. Hence, the maximized objective function of the design of SPTC, called the concentration ratio, is given by Equation (3). Equations (1)–(3) are calculated as follows:

$$f = a / [4 \tan\left(\frac{\phi_r}{2}\right)] \quad (1)$$

$$d = \frac{a^2}{16f} \quad (2)$$

$$C = \frac{a - a'}{\pi a'} \quad (3)$$

The reflector surface area and receiver diameter of the SPTC is related to its basic design parameters, and it is given by Equations (4) and (7), respectively:

$$S = \left[\frac{a}{2} \sqrt{\left(\frac{4d}{a} \right)^2 + 1} \right] + 2f \ln \left[\frac{4d}{a} + \sqrt{\left(\frac{4d}{a} \right)^2 + 1} \right] \quad (4)$$

$$p = \frac{2f}{1 + \cos \varnothing_r} \quad (5)$$

The wind impact on the trough and supporting system, the design error on the tracking mechanism, and the misplacement of the receiver tube due to the thermal expansion are the main reasons for tracking errors, leading to changes in the solar incidence angle (0 to 3°). Based on the required optimized concentration ratio of SPTC, the entire design parameters are justified, and the receiver tube diameter is always to be as small as possible, which is shown in Figure 2.

$$\tan(90 - \varnothing_r + \varnothing_a) = \frac{f - d}{\frac{a}{2} - \frac{a'}{2}} \quad (6)$$

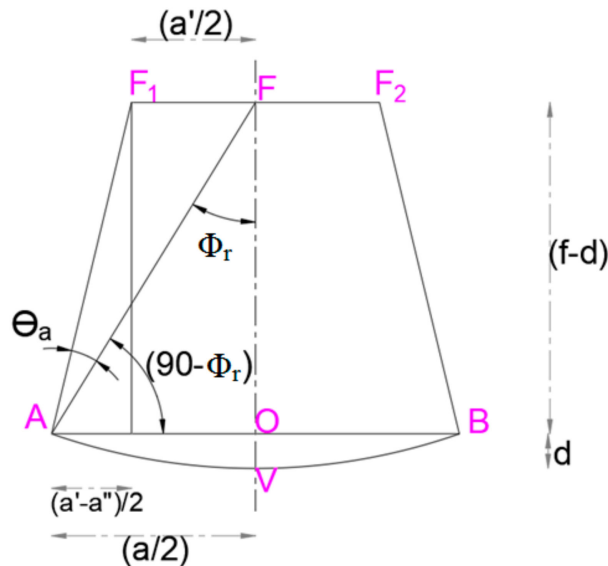


Figure 2. Geometrical design of the SPTC.

In the current design of SPTC, all the design parameters are derived as a function of the main three design parameters (aperture length of the primary reflector, solar incidence angle, and rim angle of the primary reflector). The mentioned three main design parameters are interrelated in all the designed mathematical models. The geometrical representation of the main three basic design parameters (aperture length of the primary reflector, solar incidence angle, and rim angle of the primary reflector) and the sample cross-sectional view of the SPTC is shown in Figure 3.

$$a' = a - \frac{2(f - d)}{\tan(90 - \varnothing_r + \theta_a)} \quad (7)$$

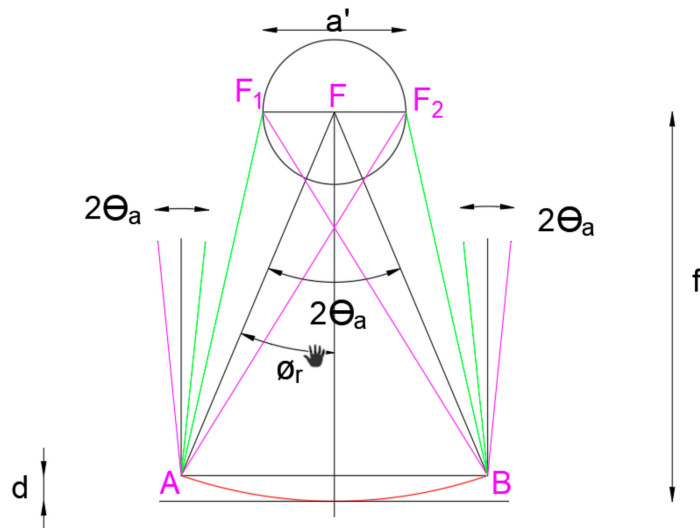


Figure 3. Cross sectional view of the SPTC.

From the basic geometrical design model of SPTC, it is very clear that the receiver tube diameter should be the maximum for a higher incidence angle. In addition, it is noted that the solar rays are perfectly reflected and focused on the receiver tube when the solar acceptance angle is less than the stated design value. If the solar acceptance angle is higher than the design value, then the solar rays are not exactly focused on the receiver tube, which leads the system design to being failure one with a less optical efficiency.

3. Design of CPC as a Secondary Reflector

A novel secondary reflector CPC is introduced for absorbing all the reflected solar rays from the parabolic trough to the receiver tube and to enhance the optical efficiency of the system. In general, CPC is a different type of solar concentrating collector made up in the shape of two intersecting parabolas. It is a kind of non-tracking solar concentrator that has the maximum possibilities for its enhancement in a concentration ratio in the large aperture area. There are various absorber contours that are currently used with a CPC for different acceptance angles. Thus, the concentration ratio can be increased significantly by the combination of CPC with SPTC, which leads to an increase in the overall optical efficiency of the system.

Similar to the design procedure of SPTC without a secondary reflector, the design parameters such as the rim angle, aperture, focus length, acceptance angle, depth distance, arc length, receiver tube diameter, and concentration ratio are considered in the design procedure of SPTC with the secondary reflector. All the design parameters of both SPTC and CPC are derived as a function of the main three basic design parameters (aperture length of the primary reflector, solar incidence angle, and rim angle of the primary reflector). The mathematical model of the acceptance angle, aperture length, and receiver diameter of the CPC with respect to the basic design parameters are given by Equations (8), (9), and (10), respectively. The geometric connections between them are shown in Figure 4. The CPC has two parabola sections in which the aperture length of the CPC is denoted as (a'), while the absorber length of the primary reflector is denoted as (a''). The relation between the focal distance and rim angle of the CPC is also to be geometrically connected to find the optimum design of CPC, which is shown in Figure 5.

$$\theta_a' = \varnothing_r - \theta_a \quad (8)$$

$$a' = a - \frac{2(f-d)}{\tan(90 - \varnothing_r + \theta_a)} \quad (9)$$

$$a'' = a' \sin(\theta_a') \quad (10)$$

$$PR = \frac{a'}{2 \sin \theta_{a'}}$$
 (11)

$$RF = \frac{a''}{2 \sin \theta_{a'}}$$
 (12)

$$PR + RF = \frac{(a' + a'')}{2 \sin \theta_{a'}}$$
 (13)

$$P' = \frac{2f}{1 + \cos \phi_r'}$$
 (14)

$$\frac{(a' + a'')}{2 \sin \theta_{a'}} = \frac{2f}{1 + \cos \phi_r'}$$
 (15)

$$\cos(180 - \phi_r') = \frac{d' - f'}{P'}$$
 (16)

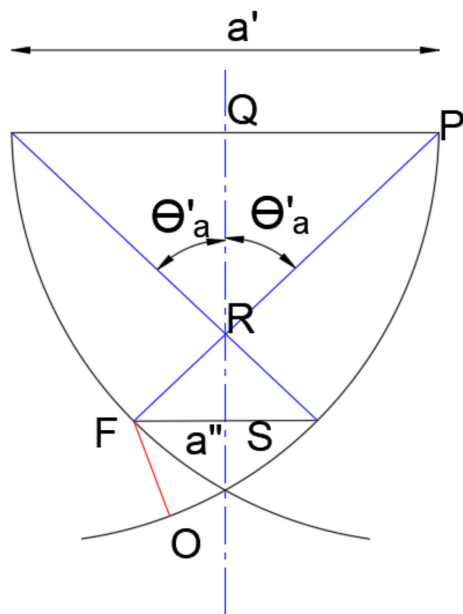


Figure 4. Acceptance angle and aperture of CPC.

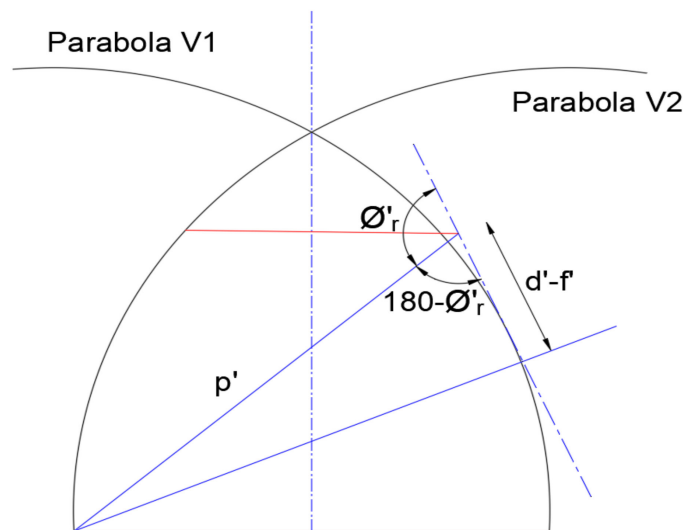


Figure 5. Rim angle of CPC.

The geometric view of CPC for extracting the relationship among the CPC design parameters with the height of the CPC collector is shown in Figure 6. The derived mathematical model of concentration ratio of the novel SPTC with the secondary reflector is shown in Equation (19), the focal length and arc length of the CPC parabolas are given by Equations (20) and (21).

$$SR = \frac{a''}{2 \tan \theta_a'} \quad (17)$$

$$RQ = \frac{a}{2 \tan \theta_a'} \quad (18)$$

$$C' = \frac{1}{\sin(\theta_a')} = \frac{a}{a'} \quad (19)$$

$$f' = \frac{a''(1 + \sin(\theta_a'))}{2} \quad (20)$$

$$s' = (1 + C')a' \quad (21)$$

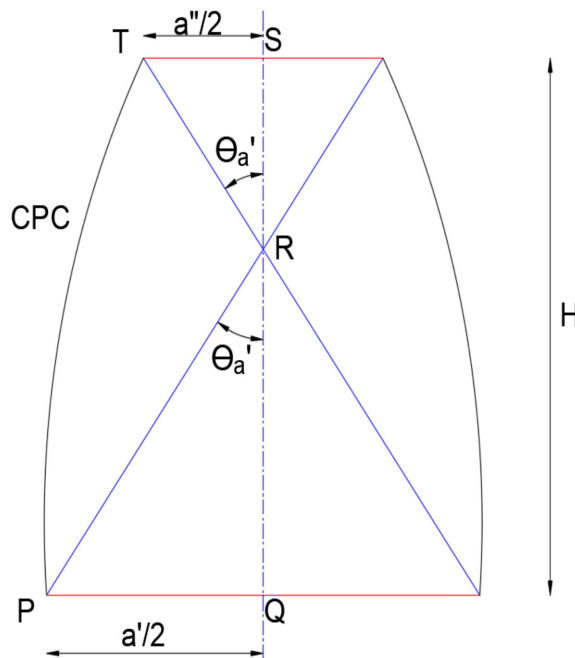


Figure 6. Geometric view of height of the CPC.

The mathematical model of the rim angle, height, and depth of the CPC is shown in Equations (22), (31), and (32), respectively. The secondary reflector height and aperture area are correlated as per the preferred aperture length of the primary collector and solar acceptance angle. The height of the CPC should be optimized for the truncated design without affecting the concentration ratio and the geometrical design of truncated CPC is shown in Figure 7.

$$\phi_r' = \cos^{-1} \left[\left(\frac{4f \sin \theta_a'}{a' + a''} \right) - 1 \right] \quad (22)$$

For the design of vertex of parabola V_1

From the triangle OQF:

$$x = f' \sin \theta_a' \quad (23)$$

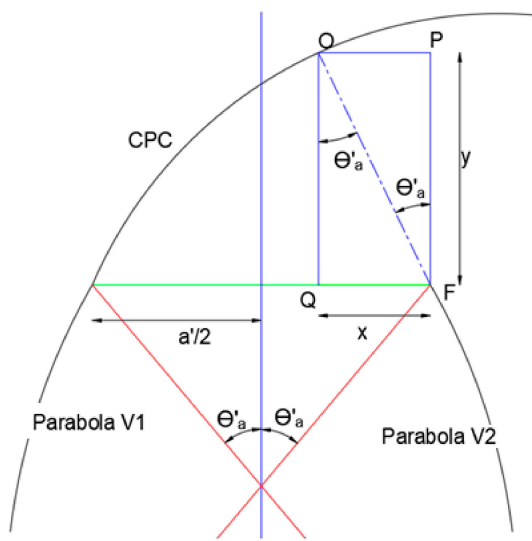


Figure 7. Geometrical view of the vertex of CPC.

x vertex is at a distance of:

$$V_{1x} = \frac{a''}{2} - x \quad (24)$$

$$V_{1x} = \frac{a''}{2} - f' \sin \theta_a' \quad (25)$$

From the triangle OPF:

$$y = f' \cos \theta_a' \quad (26)$$

y vertex is at a distance of:

$$V_{1y} = H + f + y \quad (27)$$

$$V_{1y} = H + f + f' \cos \theta_a' \quad (28)$$

Similarly, for the design of vertex of parabola V_2 :

$$V_{2x} = f' \sin \theta_a' - \frac{a''}{2} \quad (29)$$

$$V_{2y} = H + f + f' \cos \theta_a' \quad (30)$$

$$H = \frac{a' + a''}{2 \tan \theta_a'} \quad (31)$$

$$d = f' + \frac{2 f' \cos(180 - \phi_r')}{1 + \cos \phi_r'} \quad (32)$$

The optical efficiency for CPC is comparatively higher than the parabolic trough collector for the same aperture design and solar radiation. In general, the diffused radiation is not successfully collected in concentrating collectors and the solar flux contribution of diffused radiation is always inversely proportional to the concentration ratio. Thus, the main advantage of using CPC is that it can collect the maximum solar diffused radiation from available solar radiation across the aperture and its performance is also satisfactory on cloudy days. To support the uniform distribution of the solar flux and heat flux across the surface area of the receiver tube, a dual receiver tube can also be introduced for CPC collectors. The design equations of the CPC are moreover correlated with the basic design parameters and the cross-sectional model of the secondary reflector (CPC) is shown in Figure 8.

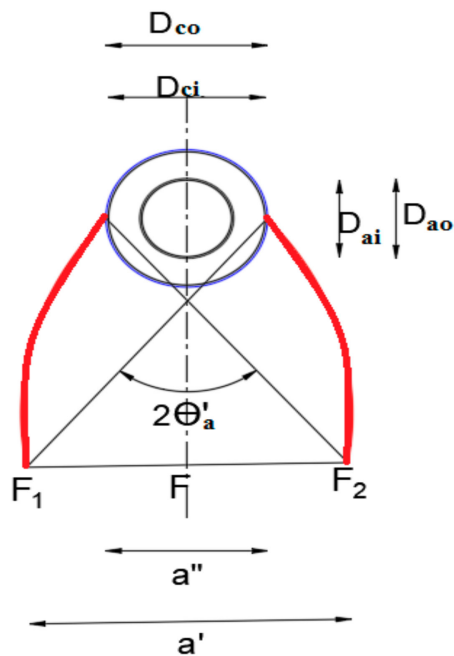


Figure 8. Cross sectional model of CPC's secondary reflector.

4. Optimization and Simulation of SPTC with and without CPC

The mathematical model of the design of SPTC and CPC are solved and optimized using MATLAB for the unit length of the collector. The optimizing conditions for solving the modeling equations are to maximize the concentration ratio and to minimize the surface area and height of the SPTC with CPC. The geometrical feasibility of the rim angle of the CPC should be more than 90° . The CPC truncated parabola is becoming flat in nature at 90° . The secondary reflector has become a convex one in nature when the rim angle is less than 90° . The optical properties of the SPTC and CPC are assumed to be steady and uniform across the reflector and absorber surfaces. The typical cross-section of the proposed design of novel SPTC with CPC is shown in Figure 9. The proposed design shows that the reflection of the solar incidence rays with error incidence angles at positive and negative vectors. The reflected rays are converged into the secondary reflector for maximum error of the incidence angle about 3° . The aperture of the SPTC is fixed as 2 m due to its technical and economic feasibility for the required design.

The total arc length of reflector surface, total height, and the overall concentration ratio of the SPTC with CPC are calculated from Equations (33), (34), and (35), respectively. The design parameters of SPTC and CPC are optimized based on the increased concentration ratio and decreased the surface area for the range of acceptance angle (0 to 3°) using MATLAB software. Equations (33)–(35) are as follows:

$$S_{\text{SPTC+CPC}} = [s + s']L \quad (33)$$

$$H' = f + H + \frac{a''}{2} \quad (34)$$

$$C_{\text{overall}} = \frac{a - a'}{a''} \quad (35)$$

The optimized design parameters of the SPTC with CPC is shown in Table 1. The optimum design parameters are evaluated from the mathematical model for the required aperture length and acceptance angle of primary collector.

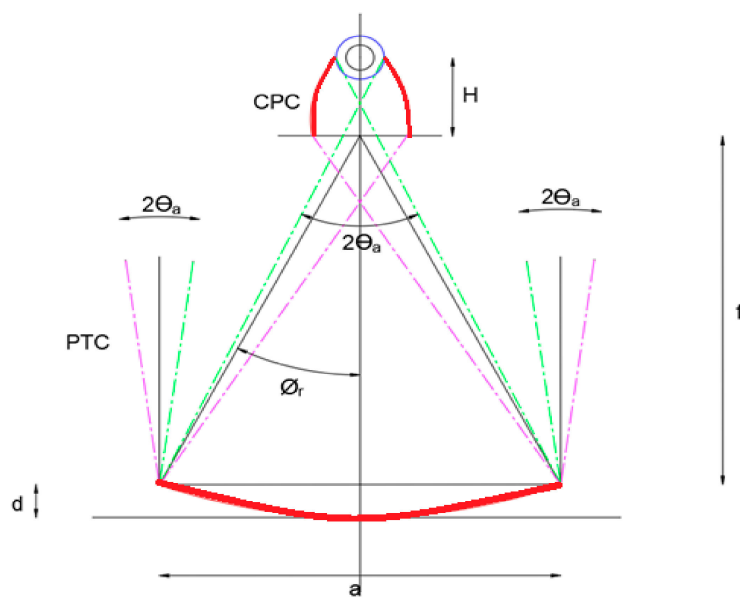


Figure 9. Cross sectional model of the SPTC with CPC.

Table 1. Technical specifications of SPTC with the secondary reflector.

Description	Symbols	Values
Aperture of primary collector	a	2 m
Rim angle of primary collector	Φ_r	30°
Maximum acceptance angle of primary collector	θ_a	2°
Focus distance of primary collector	f	1.87 m
Depth of primary collector	d	134 mm
Acceptance angle of secondary reflector	$\theta_{a'}$	28°
Aperture of secondary reflector	a'	158 mm
Height of secondary reflector	H	218 mm
Concentration ratio of secondary reflector	C'	2.13
Total surface area of SPTC	A_s	2.519 m ²
Overall Concentration ratio of SPTC	C	7.9
Absorber outer diameter	$D_{a,o}$	54 mm
Absorber inner diameter	$D_{a,i}$	50 mm
Cover outer diameter	$D_{c,o}$	74 mm
Cover inner diameter	$D_{c,i}$	70 mm
Emissivity of the cover	ϵ_c	0.85
Transmittance of the cover	τ_c	0.95
Absorptivity of the absorber	α	0.95
Reflectivity of the mirror	ρ	0.85

For finding the optimum design of SPTC without CPC from the mathematical model, the design equations of SPTC are solved using MATLAB for incidence angle of solar rays (0 to 3°). The modeled primary reflector and receiver tube of SPTC without CPC are shown in Figure 10a. The optical ray-tracing simulation performance of SPTC without CPC model is simulated using TRACE PRO software by considering the local atmospheric conditions on a day in May 2020 for the range of acceptance angles from 0 to 3°. The converging solar rays on the absorber tube and the reflected rays from the reflector are compared with the solar incident rays on the surface of the reflector of SPTC. From the simulation results, it is evident that most of the reflected rays from the primary reflector are not converging on the receiver tube due to the effect of the error on the solar incidence angle. The absorbed flux on the surface of the receiver tube is also calculated from the simulation results. The flux absorbed on the receiver tube is also very less when varying the incidence angle of solar rays from 0 to 3° as shown in Figure 10b.

Similar to the optimized design of SPTC without CPC, the optimized design of SPTC with CPC is evaluated using MATLAB by considering the error in the tracking system for the solar incidence angle (0 to 3°). The optimized designs of the primary reflector, secondary reflector, and receiver tube of SPTC with a secondary reflector is shown in Figure 10c. The optical ray-tracing simulation on TRACE PRO software is performed on the SPTC with the secondary reflector model by considering the local atmospheric conditions on a day in May 2020 for the range of solar incidence angle (0 to 3°), as shown in Figure 10d. It is found that the receiver tube of SPTC with CPC absorbs the maximum reflected rays, which are not converged in the SPTC without CPC in the previous case.

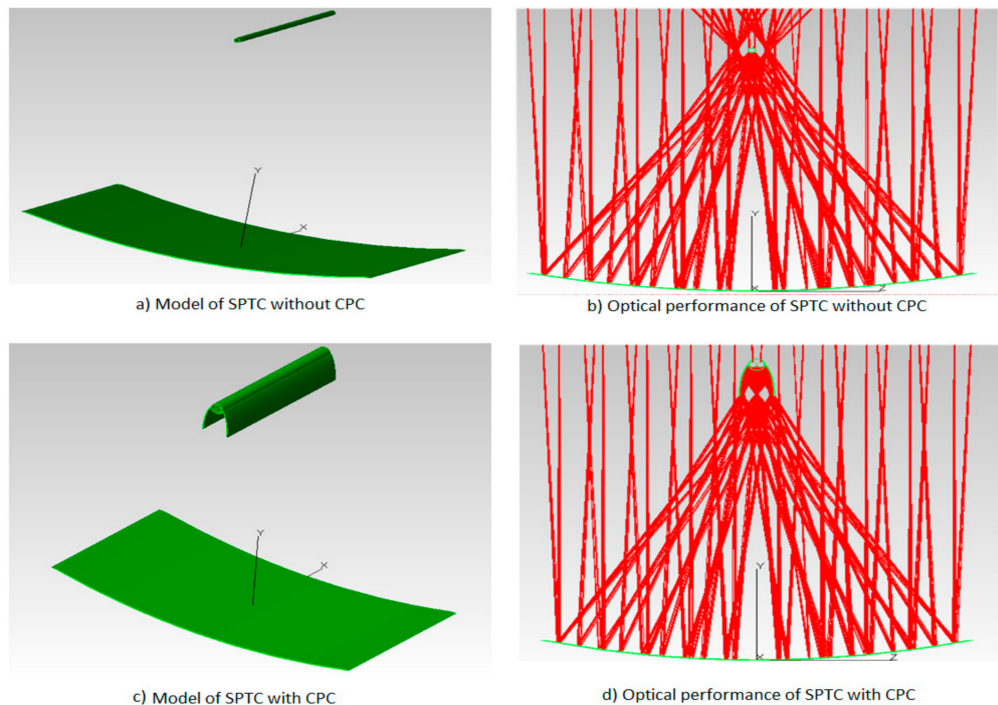


Figure 10. Modelling and simulation of optical performance of SPTC in TRACEPRO.

5. Results and Discussion

By varying the incidence angle of solar rays and the rim angle of the primary reflector, the design parameters of both SPTC and CPC are optimized using MATLAB simulations. The effect of the incidence angle (0.5° to 3°) and rim angle (25° to 60°) investigations on the design of aperture length of CPC is carried out, and it is optimized for its minimum value as shown in Figure 11a. The reason for the minimum aperture length of CPC is to avoid the interruption of the beam solar rays that are hitting the primary reflector. Since some of the solar rays are not hitting the primary reflector due to the presence of a secondary reflector, the aperture length of CPC should be minimized as much as possible. The aperture length is increased because of increasing the rim angle initially, then the aperture length tends to decrease. From the result, it is worth mentioning that the aperture length is very minimum at 45° rim angle and all the incidence angles of SPTC. Similar to the aperture length, the receiver diameter of CPC needs to be optimized by varying incidence angle of solar rays and rim angle of the primary reflector. The optimized results are shown in Figure 11b. From the results, it is found that the increment in the solar incidence angle due to imperfect tracking of SPTC towards the sun movement leads to an increase in the receiver tube diameter. This significant increment on the SPTC receiver diameter reduces the concentration ratio of the collector, which leads to a reduced outlet temperature of the working fluid. Therefore, the receiver diameter should be optimized based on the maximum value of the concentration ratio. The noteworthy effect of the rim angle of the primary reflector on the receiver tube diameter is also noted. The range of

receiver tube diameter for different incidence angles at lower rim angle is considerably small as compared to the higher rim angle. Hence, it is noted that the rim angle should be minimized for a higher concentration ratio.

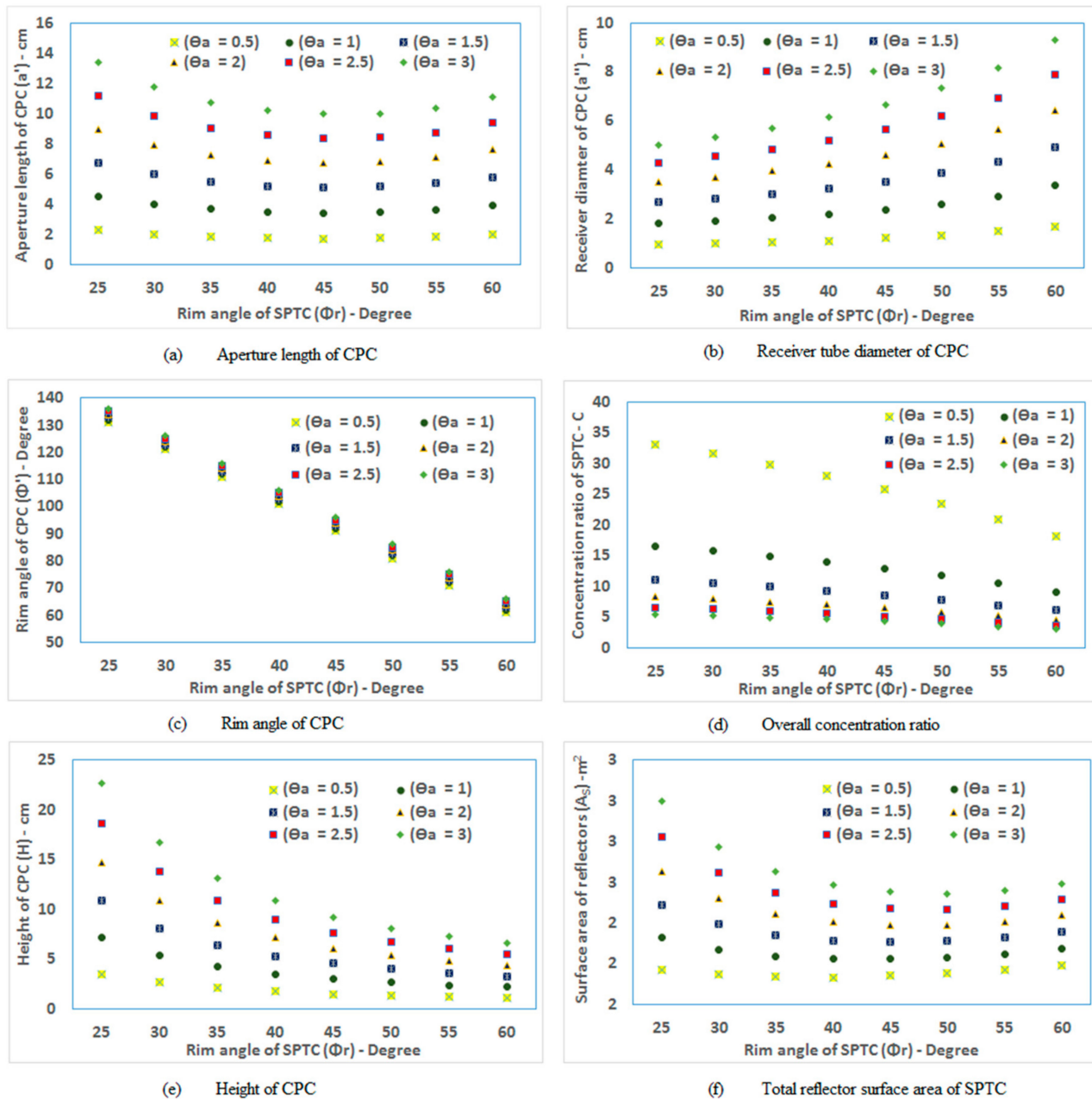


Figure 11. Optimum design parameters of SPTC with CPC for the solar incidence angle of 2 degrees.

The rim angle of the CPC is analyzed, and it is shown in Figure 11c. From the result, it is found that the rim angle of the CPC is inversely proportional to the rim angle of SPTC. The technical feasibility of the rim angle of CPC is already discussed, and the required minimum angle is 90° . It is essential to keep the rim angle of the SPTC lower than 45° for providing the CPC as a secondary reflector over the SPTC primary reflector. The significance of the incidence angle of solar rays and the rim angle of the primary reflector on the overall concentration ratio of the SPTC with the secondary reflector is also optimized, as shown in Figure 11d. From the results, it is evident that the concentration ratio is inversely proportional to the rim angle of the primary collector. For the superior fluid

outlet temperature, it is distinguished that the system should have a higher concentration ratio. It is noted that the rim angle should be less than 45° and the same has to be nominated for a redesign of the SPTC system.

The height of the CPC secondary reflector should be calculated and minimized to avoid the shading effect on the primary collector, wind impact on the supporting systems, and effective tracking. The height of CPC is progressively reducing when increasing the rim angle, as shown in Figure 11e. Therefore, the higher rim angle is preferred for lower height CPC collectors, but at the same time, the total surface area of the reflectors with respect to the rim angle should be investigated. The overall reflector area of the collector is gradually decreasing and then increasing with respect to the rim angle increment of SPTC, as shown in Figure 11f. The reflector surface area should be minimized, and it is optimized for the range of rim angle of the primary collector about 30° to 40°. The design parameters such as the receiver tube diameter of CPC, the aperture of CPC, the rim angle of CPC, the overall concentration ratio of SPTC, the height of CPC, and the total reflector surface area are investigated with respect to the rim angle and the acceptance angle of the primary reflector for the fixed aperture of the primary reflector. In addition, it is noted from the optimization results that the design parameters should be optimized for a particular range of acceptance angles of the primary reflector for better optical performance.

To distinguish the significance of providing the secondary reflector for SPTC, it is essential to analyze the amount of flux that is actually focused on the receiver tube from the SPTC with and without a secondary reflector. The optimized design of the SPTC is modeled in the MATLAB and the following Equations (36) and (37) are used for computing the ideal solar flux received on the absorber of the SPTC with and without a secondary reflector, respectively, and without considering the tracking error and deviations in the incidence angle:

$$S_{PTC} = \frac{I_{bt}r_b\tau\alpha[a' + \rho(a - a')]}{\pi a'} \quad (36)$$

$$S_{PTC+CPC} = \frac{I_{bt}r_b\tau\alpha[a'' + \rho\rho'(a - a'')]}{\pi a''} \quad (37)$$

The solar absorbed flux on the receiver tube is noted from the TRACEPRO simulation results with respect to the optimized design conditions of SPTC with and without a secondary reflector. The effect of tracking error and deviations in the incidence angle on the performance of SPTC with and without CPC is carried out, and the typical simulation result is shown in Figure 12a. The absorbed flux on the receiver tube of SPTC from the simulation results with the radiation values for an entire day at different configurations (with and without CPC, with and without tracking error) of SPTC is shown in Figure 12b. Solar radiation for the respective day, solar absorbed flux, and optical efficiency are represented in Table 2.

In the simulation of the SPTC with the secondary reflector it is evident that the presence of the CPC secondary reflector significantly increases the absorbed flux and the flux distribution. The flux distribution is maximum at both edges of the receiver tube due to the nature of CPC, meanwhile two parabolas are reflecting the rays to both of its focus. The radiation is noted from the weather station for a day in May 2020, which ranges from 125 to 838 W/m². The range of absorbed solar flux for the SPTC without a secondary reflector is 400 to 2600 W/m², and the average flux is 1600 W/m² for a perfect reflecting nature of the tracking mechanism without any error in the solar incidence angle. Meanwhile, the range of the absorbed solar flux for the SPTC with a secondary reflector is 700 to 4700 W/m², and the average flux is 2900 W/m². The receiver tube diameter of CPC is smaller than the receiver tube diameter of the SPTC without a secondary reflector. Therefore, the flux is higher for a smaller surface of the receiver tube. Hence, the concentration ratio can be improved for achieving the higher outlet fluid temperature.

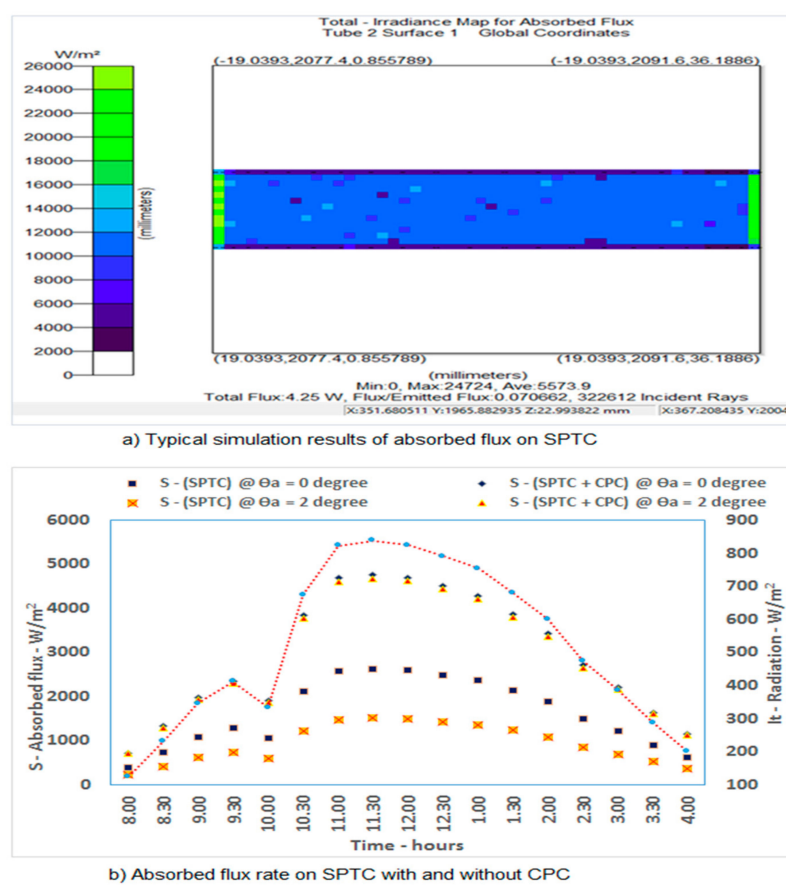


Figure 12. Absorbed flux on receiver tube surface of SPTC for different configurations.

Table 2. Radiation, absorbed flux, optical efficiency of SPTC with and without CPC for ideal and actual tracking conditions.

Time	I _t	Absorbed Solar Flux on the Receiver Tube				Optical Efficiency			
		S – (SPTC) @ θ _a = 0°	S – (SPTC + CPC) @ θ _a = 0°	S – (SPTC) @ θ _a = 2°	S – (SPTC + CPC) @ θ _a = 2°	η ₀ – (SPTC) @ θ _a = 0°	η ₀ – (SPTC + CPC) @ θ _a = 0°	η ₀ – (SPTC) @ θ _a = 2°	η ₀ – (SPTC + CPC) @ θ _a = 2°
(h)	W/m ²	W/m ²	W/m ²	W/m ²	W/m ²	%	%	%	%
8.00	125	391.95	711.53	224.79	699.45	0.7778	0.6613	0.4461	0.6501
8.30	232	727.46	1320.60	419.28	1293.19	0.7778	0.6613	0.4483	0.6476
9.00	345	1081.79	1963.82	621.55	1927.22	0.7778	0.6613	0.4469	0.6490
9.30	411	1288.74	2339.50	741.94	2292.73	0.7778	0.6613	0.4478	0.6481
10.00	334	1047.29	1901.20	603.61	1861.75	0.7778	0.6613	0.4483	0.6476
10.30	674	2113.40	3836.56	1215.62	3767.97	0.7778	0.6613	0.4474	0.6495
11.00	822	2577.47	4679.01	1479.90	4586.87	0.7778	0.6613	0.4466	0.6483
11.30	838	2627.64	4770.08	1511.41	4677.60	0.7778	0.6613	0.4474	0.6485
12.00	825	2586.88	4696.09	1486.97	4614.26	0.7778	0.6613	0.4471	0.6498
12.30	790	2477.13	4496.86	1423.25	4431.43	0.7778	0.6613	0.4469	0.6517
1.00	753	2361.11	4286.25	1359.63	4205.73	0.7778	0.6613	0.4479	0.6489
1.30	680	2132.22	3870.71	1228.64	3790.98	0.7778	0.6613	0.4482	0.6477
2.00	601	1884.50	3421.03	1086.63	3349.00	0.7778	0.6613	0.4485	0.6474
2.30	475	1489.42	2703.81	857.09	2646.48	0.7778	0.6613	0.4476	0.6473
3.00	386	1210.35	2197.20	695.25	2159.91	0.7778	0.6613	0.4468	0.6501
3.30	288	903.06	1639.36	520.36	1610.55	0.7778	0.6613	0.4482	0.6497
4.00	200	627.12	1138.44	361.20	1117.06	0.7778	0.6613	0.4480	0.6489

The ideal optical efficiency of the SPTC without and with secondary reflector are calculated from Equations (38) and (39), respectively:

$$\eta_{o,PTC} = \frac{S_{PTC}(\pi a')}{I_{bt}(a)} \quad (38)$$

$$\eta_{o,PTC+CPC} = \frac{S_{PTC+CPC}(\pi a'')}{I_{bt}(a)} \quad (39)$$

The ideal optical efficiency of the SPTC with and without a secondary reflector for an incidence angle at 0° is calculated as 77% and 66%, respectively. Deviations in conflicting mode at ideal conditions reveal that the secondary reflector is once again reflecting the reflected solar rays into the absorber tube with its own optical loss due to its reflectivity. This secondary reflection leads to decreases the rate of optical energy and it is noticed that the secondary reflector may not be a suitable choice for SPTC with a perfect tracking system. However, in practical, the tracking error is always there, and the rate of the error in the solar incidence angle is always at a transient state with respect to the ambient conditions. In addition, the rate of the average absorbed flux is comparatively higher for the SPTC with CPC than the SPTC without CPC, which leads to an enhancement of the thermal performance of the system.

The novel design and mathematical model of SPTC without and with a secondary reflector are validated using TRACEPRO and MATLAB simulations, and their results are shown in Figure 13a,b, respectively. For a tracking deviation of 2° in the solar incidence angle, the average absorbed solar flux for the SPTC without a secondary reflector is 900 W/m^2 for the range of 200 to 1500 W/m^2 . It is also observed that only 58% of the solar rays are reflected in the focus and the remaining 42% of the rays are lost due to the tracking deviation on the focusing. To overcome these optical losses in the system, a novel secondary reflector is designed, and it is investigated for the enhancement of its optical performance. The simulation result shows that the range of absorbed solar flux for the SPTC with the secondary reflector is 700 to 4600 W/m^2 and the average flux is 2800 W/m^2 . The optical efficiency of the SPTC with and without secondary reflector for incidence angle at 2° is also calculated as 45% and 65%, respectively. The maximum available solar energy for a typical day is received by SPTC with and without CPC for tracking the deviation in the solar incidence angle of 2° is 19.30 MJ and 13.14 MJ, respectively, for the full day solar radiation of 29.75 MJ.

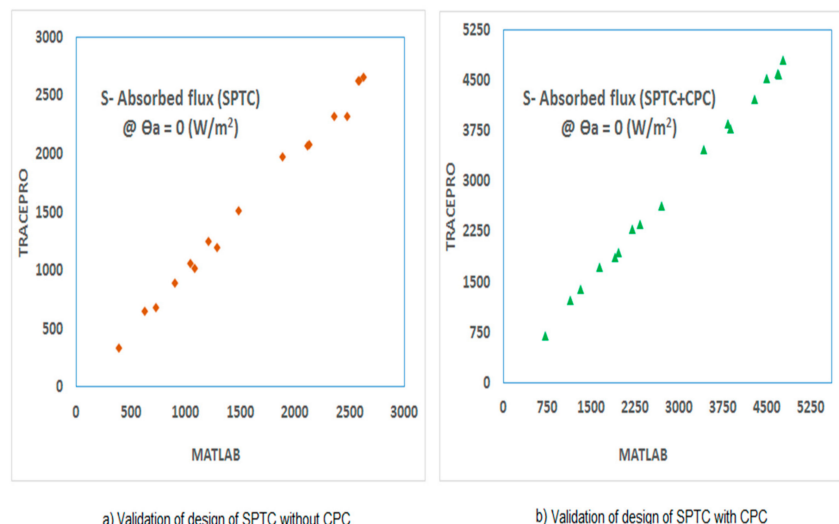


Figure 13. Validation of the mathematical model of SPTC using MATLAB and TRACEPRO.

6. Conclusions

The numerical investigations for evaluating the optical performance of SPTC with and without secondary reflector have been performed. An analysis was conducted by varying the rim angle of the primary reflector of SPTC and varying the incidence angle of the solar rays. The optimum rim angle of primary reflector was found to be 30° for different incidence angles of solar rays in the design of the CPC. The optical performance of the SPTC with and without the CPC was carried out and compared with an average absorbed flux obtained from MATLAB and TRACE PRO software. The absorbed flux on the surface of the receiver tube was found to be the maximum value for SPTC with secondary reflector at a tracking error of 2° . The result shows that the average flux on the receiver tube of SPTC with CPC is 111% higher than the SPTC without CPC. The optical efficiency of the SPTC is increased by 20% by incorporating a secondary reflector. The proposed SPTC with CPC can be implemented to avoid the optical losses due to error in single axis tracking systems.

Author Contributions: Conceptualization, C.S.; methodology, C.S., and J.S.; software, C.S. and N.A.; validation, C.S., B.K. and N.A.; investigation, C.S. and J.S.; resources, N.P. and T.S.; writing—original draft preparation, C.S., J.S. and B.K.; writing—review and editing, C.S., B.K. and N.P.; visualization, C.S. and J.S.; supervision, T.Y., N.A. and T.S.; formal analysis, N.P. and T.S.; project administration, T.Y. and N.P.; funding acquisition, T.S. All authors have read and agreed to the published version of the manuscript.

Funding: This research received no external funding.

Institutional Review Board Statement: Not applicable.

Informed Consent Statement: Not applicable.

Data Availability Statement: The data presented in this study is available within the article.

Conflicts of Interest: The authors declare no conflict of interest.

Nomenclature

a	Aperture of PTC, m
Φ_r	Rim angle of PTC, degree
θ_a	Acceptance angle of PTC, degree
f	Focal length of PTC, m
d	Depth of PTC, m
s	Arc length of PTC, m
$\theta_{a'}$	Acceptance angle in CPC, degree
a'	Aperture of CPC, m
a''	Receiver length of CPC, m
A_s	Surface area of the collector, m^2
$\Phi_{r'}$	Rim angle of CPC, degree
f'	Focal length of CPC, m
s'	Arc length of CPC, m
H	Height of CPC, m
C	Concentration ratio
C'	Concentration ratio (CPC)
Coverall	Concentration ratio (CPC)
$S - SPTC$	Absorbed Flux of SPTC without CPC, W/m^2
$S - SPTC + CPC$	Absorbed Flux of SPTC with CPC, W/m^2
Ibt	Beam radiation, W/m^2
$H(o, PTC)$	Optical efficiency of SPTC without CPC, %
$\eta(o, PTC+CPC)$	Optical efficiency of SPTC with CPC, %
ϵ	Emissivity

τ	Transmissivity
α	Absorptivity
ρ	Reflectivity of the primary reflector
ρ''	Reflectivity of the secondary reflector

References

- Jain, A.; Das, P.; Yamujala, S.; Bhakar, R.; Mathur, J. Resource potential and variability assessment of solar and wind energy in India. *Energy* **2020**, *211*, 118993. [\[CrossRef\]](#)
- Subramani, J.; Nagarajan, P.K.; Mahian, O.; Sathyamurthy, R. Efficiency and heat transfer improvements in a parabolic trough solar collector using TiO_2 nanofluids under turbulent flow regime. *Renew. Energy* **2018**, *119*, 19–31. [\[CrossRef\]](#)
- Subramani, J.; Nagarajan, P.K.; Wongwises, S.; El-Agouz, S.A.; Sathyamurthy, R. Experimental study on the thermal performance and heat transfer characteristics of solar parabolic trough collector using Al_2O_3 nanofluids. *Environ. Prog. Sustain. Energy* **2018**, *37*, 1149–1159. [\[CrossRef\]](#)
- Barbosa, E.G.; Martins, M.A.; Viana de Araujo, M.E.; dos Santos Renato, N.; Zolnier, S.; Pereira, E.G.; de Oliveira Resende, M. Experimental evaluation of a stationary parabolic trough solar collector: Influence of the concentrator and heat transfer fluid. *J. Clean. Prod.* **2020**, *276*, 124174. [\[CrossRef\]](#)
- Qin, C.; Kim, J.B.; Lee, B.J. Performance analysis of a direct-absorption parabolic-trough solar collector using plasmonic nanofluids. *Renew. Energy* **2019**, *143*, 24–33. [\[CrossRef\]](#)
- Fathabadi, H. Novel low-cost parabolic trough solar collector with TPCT heat pipe and solar tracker: Performance and comparing with commercial flat-plate and evacuated tube solar collectors. *Sol. Energy* **2020**, *195*, 210–222. [\[CrossRef\]](#)
- Senthil Manikandan, K.; Kumaresan, G.; Velraj, R.; Iniyan, S. Parametric study of solar Parabolic Trough Collector system. *Asian J. Appl. Sci.* **2012**, *5*, 384–393. [\[CrossRef\]](#)
- Bellos, E.; Tzivanidis, C. Investigation of a star flow insert in a parabolic trough solar collector. *Appl. Energy* **2018**, *224*, 86–102. [\[CrossRef\]](#)
- Bitam, E.W.; Demagh, Y.; Hachicha, A.A.; Benmoussa, H.; Kabar, Y. Numerical investigation of a novel sinusoidal tube receiver for parabolic trough technology. *Appl. Energy* **2018**, *218*, 494–510. [\[CrossRef\]](#)
- Hafez, A.Z.; Attia, A.M.; Eltwab, H.S.; ElKousy, A.O.; Afifi, A.A.; AbdElhamid, A.G.; AbdElqader, A.N.; Fateen, S.E.K.; El-Metwally, K.A.; Soliman, A.; et al. Design analysis of solar parabolic trough thermal collectors. *Renew. Sustain. Energy Rev.* **2018**, *82*, 1215–1260. [\[CrossRef\]](#)
- Bellos, E.; Tzivanidis, C. Alternative designs of parabolic trough solar collectors. *Prog. Energy Combust. Sci.* **2019**, *71*, 81–117. [\[CrossRef\]](#)
- Malan, A.; Ravi Kumar, K. A comprehensive review on optical analysis of parabolic trough solar collector. *Sustain. Energy Technol. Assess.* **2021**, *46*, 101305. [\[CrossRef\]](#)
- Li, X.; Chang, H.; Duan, C.; Zheng, Y.; Shu, S. Thermal performance analysis of a novel linear cavity receiver for parabolic trough solar collectors. *Appl. Energy* **2019**, *237*, 431–439. [\[CrossRef\]](#)
- Zhao, Z.; Bai, F.; Zhang, X.; Wang, Z. Experimental study of pin finned receiver tubes for a parabolic trough solar air collector. *Sol. Energy* **2020**, *207*, 91–102. [\[CrossRef\]](#)
- Yilmaz, I.H.; Mwesigye, A.; Göksu, T.T. Enhancing the overall thermal performance of a large aperture parabolic trough solar collector using wire coil inserts. *Sustain. Energy Technol. Assess.* **2020**, *39*, 100696. [\[CrossRef\]](#)
- Hatami, M.; Geng, J.; Jing, D. Enhanced efficiency in Concentrated Parabolic Solar Collector (CPSC) with a porous absorber tube filled with metal nanoparticle suspension. *Green Energy Environ.* **2018**, *3*, 129–137. [\[CrossRef\]](#)
- Pranesh, V.; Velraj, R.; Christopher, S.; Kumaresan, V. A 50 year review of basic and applied research in compound parabolic concentrating solar thermal collector for domestic and industrial applications. *Sol. Energy* **2019**, *187*, 293–340. [\[CrossRef\]](#)
- Acosta-Herazo, R.; Valadés-Pelayo, P.J.; Mueses, M.A.; Pinzón-Cárdenas, M.H.; Arancibia-Bulnes, C.; Machuca-Martínez, F. An optical and energy absorption analysis of the solar compound parabolic collector photoreactor (CPCP): The impact of the radiation distribution on its optimization. *Chem. Eng. J.* **2020**, *395*, 125065. [\[CrossRef\]](#)
- Kurhe, N.; Pathak, A.; Deshpande, K.; Jadkar, S. Compound parabolic solar collector—Performance evaluation as per standard test method and actual field conditions for industrial process heat application in Indian context. *Energy Sustain. Dev.* **2020**, *57*, 98–108. [\[CrossRef\]](#)
- Manikandan, G.K.; Iniyan, S.; Goic, R. Enhancing the optical and thermal efficiency of a parabolic trough collector—A review. *Appl. Energy* **2019**, *235*, 1524–1540. [\[CrossRef\]](#)
- Jamali, H. Investigation and review of mirrors reflectance in parabolic trough solar collectors (PTSCs). *Energy Rep.* **2019**, *5*, 145–158. [\[CrossRef\]](#)
- Bellos, E.; Tzivanidis, C. Investigation of a booster secondary reflector for a parabolic trough solar collector. *Sol. Energy* **2019**, *179*, 174–185. [\[CrossRef\]](#)
- Gong, J.-H.; Wang, J.; Lund, P.D.; Hu, E.-Y.; Xu, Z.-C.; Liu, G.-P.; Li, G.-S. Improving the performance of a 2-stage large aperture parabolic trough solar concentrator using a secondary reflector designed by adaptive method. *Renew. Energy* **2020**, *152*, 23–33. [\[CrossRef\]](#)

24. Reddy, K.S.; Singla, H.; Natraj. Gravity & wind load analysis and optical study of solar parabolic trough collector with composite facets using optimized modelling approach. *Energy* **2019**, *189*, 116065. [[CrossRef](#)]
25. Xu, L.; Sun, F.; Ma, L.; Li, X.; Lei, D.; Yuan, G.; Zhu, H.; Zhang, Q.; Xu, E.; Wang, Z. Analysis of optical and thermal factors' effects on the transient performance of parabolic trough solar collectors. *Sol. Energy* **2019**, *179*, 195–209. [[CrossRef](#)]
26. Prahl, C.; Röger, M.; Stanicki, B.; Hilgert, C. Absorber tube displacement in parabolic trough collectors—A review and presentation of an airborne measurement approach. *Sol. Energy* **2017**, *157*, 692–706. [[CrossRef](#)]
27. Canavarro, D.; Chaves, J.; Collares-Pereira, M. New second-stage concentrators (XX SMS) for parabolic primaries; Comparison with conventional parabolic trough concentrators. *Sol. Energy* **2013**, *92*, 98–105. [[CrossRef](#)]
28. Reddy, K.S.; Balaji, S.; Sundararajan, T. Estimation of heat losses due to wind effects from linear parabolic secondary reflector–receiver of solar LFR module. *Energy* **2018**, *150*, 410–433. [[CrossRef](#)]
29. Balghouthi, M.; Ali, A.B.H.; Trabelsi, S.E.; Guizani, A. Optical and thermal evaluations of a medium temperature parabolic trough solar collector used in a cooling installation. *Energy Convers. Manag.* **2014**, *86*, 1134–1146. [[CrossRef](#)]
30. Sallaberry, F.; De Jalón, A.G.; Torres, J.L.; Pujol-Nadal, R. Optical losses due to tracking error estimation for a low concentrating solar collector. *Energy Convers. Manag.* **2015**, *92*, 194–206. [[CrossRef](#)]